AGU PUBLICATIONS

Water Resources Research

RESEARCH ARTICLE

10.1002/2013WR013806

Key Points:
- A probabilistic sediment cascade model of a debris flow catchment is developed
- Sediment storage (history) and triggering (climate) are key for sediment yield
- Debris flows are simulated for a wide range of rainfall intensities

Correspondence to:
P. Molnar,
molnar@ifu.baug.ethz.ch

Citation:
Bennett, G. L., P. Molnar, B. W. McArdell, and P. Burlando (2014), A probabilistic sediment cascade model of sediment transfer in the Illgraben, *Water Resour. Res.*, *50*, 1225–1244, doi:10.1002/2013WR013806.

Received 11 MAR 2013
Accepted 16 JAN 2014
Accepted article online 22 JAN 2014
Published online 14 FEB 2014

A probabilistic sediment cascade model of sediment transfer in the Illgraben

G. L. Bennett[1,2], P. Molnar[1], B. W. McArdell[3], and P. Burlando[1]

[1]Institute of Environmental Engineering, ETH Zurich, Zurich, Switzerland, [2]Now at Department of Geological Sciences, University of Oregon, Eugene, Oregon, USA, [3]Swiss Federal Institute of Forest, Snow and Landscape Research, Birmensdorf, Switzerland

Abstract We present a probabilistic sediment cascade model to simulate sediment transfer in a mountain basin (Illgraben, Switzerland) where sediment is produced by hillslope landslides and rockfalls and exported out of the basin by debris flows and floods. The model conceptualizes the fluvial system as a spatially lumped cascade of connected reservoirs representing hillslope and channel storages where sediment goes through cycles of storage and remobilization by surface runoff. The model includes all relevant hydrological processes that lead to runoff formation in an Alpine basin, such as precipitation, snow accumulation, snowmelt, evapotranspiration, and soil water storage. Although the processes of sediment transfer and debris flow generation are described in a simplified manner, the model produces complex sediment discharge behavior which is driven by the availability of sediment and antecedent wetness conditions (system memory) as well as the triggering potential (climatic forcing). The observed probability distribution of debris flow volumes and their seasonality in 2000–2009 are reproduced. The stochasticity of hillslope sediment input is important for reproducing realistic sediment storage variability, although many details of the hillslope landslide triggering procedures are filtered out by the sediment transfer system. The model allows us to explicitly quantify the division into transport and supply-limited sediment discharge events. We show that debris flows may be generated for a wide range of rainfall intensities because of variable antecedent basin wetness and snowmelt contribution to runoff, which helps to understand the limitations of methods based on a single rainfall threshold for debris flow initiation in Alpine basins.

1. Introduction

Mountain basin sediment discharge is inherently nonlinear and stochastic in its relationship to climatic forcing and sediment production. This leads to difficulties in the prediction of sediment discharge and making inferences about environmental change from sediment yield data alone [e.g., *Jerolmack and Paola*, 2010; *Van De Wiel and Coulthard*, 2010]. The nonlinearity in sediment discharge may arise from several sources, of which storage effects, geomorphic thresholds, and connectivity are generally thought to be the most important [e.g., *Walling*, 1983; *Phillips*, 2003, 2006]. Transient sediment storage in various landscape compartments (hillslopes, debris cones, river terraces, etc.) determines the availability of sediment for transport and as a result sediment discharge may be transport or supply limited [e.g., *Bovis and Jakob*, 1999; *Lisle and Church*, 2002; *Otto et al.*, 2009]. Geomorphic thresholds are tipping points in the system at which events take place or the system behavior changes either by internal adjustment or external forcing [e.g., *Schumm*, 1979]. Hydrological connectivity of sediment sources to channels modulates sediment delivery and its distribution in time and space [e.g., *Reid et al.*, 2007; *Fryirs*, 2013]. And finally stochasticity in climate, in the processes of sediment production, the mobilization of grains and pathways they follow in the landscape, all lead to an inherent variability and uncertainty in sediment transport and limit deterministic predictions [e.g., *Benda and Dunne*, 1997, *Fuller et al.*, 2003; *Malmon et al.*, 2003].

The aim of this paper is to implement the effects of storage, thresholds, and connectivity in a simple conceptual model of sediment transfer with which the nonlinearity and stochasticity in sediment discharge can be captured. The model is based on the notion of a sediment cascade, which conceptualizes the fluvial system as a cascade of connected reservoirs representing different landscape compartments (e.g., hillslopes and channels) where sediment goes through multiple cycles of storage and remobilization before being discharged from the basin [see *Burt and Allison*, 2010, and references therein]. The transfer of sediment is determined by

fluvial processes and sediment storage, while the triggering of events supplying sediment may be stochastic or related to climatic variables. This conceptualization is founded on observations which have shown debris flows to be triggered by rainfall and conditioned on basin wetness [e.g., *Badoux et al*., 2009], yet at the same time limited by the availability of sediment [e.g., *Bovis and Jakob*, 1999; *Jakob et al*., 2005]. The application presented in this paper is intended for a mountain basin where sediment is produced by hillslope landslides and exported out of the basin by floods and debris flows generated by runoff in the channels.

Numerical modeling is a useful tool for understanding and developing hypotheses about mountain basin sediment transfer because it allows for full control over initial conditions and parameters, which is difficult to achieve in either field or laboratory studies [*Van De Wiel et al*., 2011]. Sediment transfer modeling approaches range from simple empirical sediment budget models to complex physically based models that attempt to represent the processes of sediment transfer in as much detail as possible, such as landscape evolution (long term) and soil erosion (short term) models based on the 1-D or 2-D application of equations of motion for water and sediment. While they can be used for detailed simulations in space and time of sediment transfer through the drainage basin [e.g., *Coulthard et al*., 2000; *Tucker et al*., 2001; *Molnar et al*., 2006; *Coulthard and Van De Wiel*, 2007; *Van De Wiel and Coulthard*, 2010], they assume sediment transport laws and are heavily data dependent. As such they are subject to uncertainties that are difficult to evaluate, leading to an overparameterized problem where observed data are sometimes not sufficient to justify the model complexity.

Our intention in this paper is to develop a model that is lumped in space and incorporates the minimum process representation required to reproduce first-order properties of sediment transfer in a mountain basin, such as sediment discharge volumes, event frequency, residence times, and their statistical properties. A key element is the use of the modeling approach in a probabilistic framework, allowing for stochasticity in landslide triggering and reconstructing the resulting probability distributions of sediment discharge by floods and debris flows from system behavior. This inverse approach has been used for instance for avalanche modeling [*Ancey et al*., 2003]. It allows us to include the inherent uncertainty in sediment input and its effect on sediment discharge, which would not be possible with deterministic models. Some other examples of this approach in geomorphology can be found in *Benda and Dunne* [1997], *Fuller et al*. [2003], *Tipper* [2007], *Van De Wiel et al*. [2011], among others. We propose that the value of this modeling approach comes from its compatibility with available observations, the inclusion of uncertainty and randomness in sediment production and transport, and the suitability for scenario analysis.

Although in the development of the sediment cascade model in this paper we specifically have a landslide and debris flow catchment in mind, the concepts are generally applicable to any basin that can be schematized into a cascade system , e.g. see *Lu et al.* [2005, 2006] for an application to explain the sediment delivery ratio. We apply the model to the Illgraben in Switzerland, where a unique continuous 10 year record of debris flows provides the opportunity to calibrate it. In addition to the record of sediment discharge, the probability distribution of landslide volumes for the catchment has been estimated [*Bennett et al*., 2012], and there are estimates of erosion and storage of sediment on the hillslopes and in the channel [*Berger et al*., 2011; *Bennett et al*., 2013], as well as all necessary climate data. The hillslope-channel cascade approach has been qualitatively described in the Illgraben by *Bardou and Jaboyedoff* [2008], including important debris flow generating mechanisms [*Bardou and Delaloye*, 2004; *Badoux et al*., 2009]. Importantly, previous studies in the catchment enable the independent estimation of the majority of model parameters such that calibration of the model does not involve extensive fine tuning.

We have three main objectives in this paper: (1) We develop the concept and apply the sediment cascade model to the Illgraben and investigate the conditions that lead to the transformation of the probability distribution of slope failures into that of debris flows in terms of the stochastic triggering and sediment transport mechanisms in the basin. (2) We investigate the impact of sediment storage in the Illgraben cascade on simulated sediment discharge events in general, and their division into transport and supply-limited events. (3) Our premise is that the storage and availability of water and sediment (system memory) and triggering potential (climate) drive sediment discharge behavior. On this basis, we investigate the rainfall that leads to debris flows in the model in order to understand and quantify the limitations of rainfall intensity thresholds for debris flow initiation. Although our application is based only on the Illgraben, we attempt to present the approach and results in a general way, inviting comparisons with any mountain basin with similar hydrological and geomorphological processes.

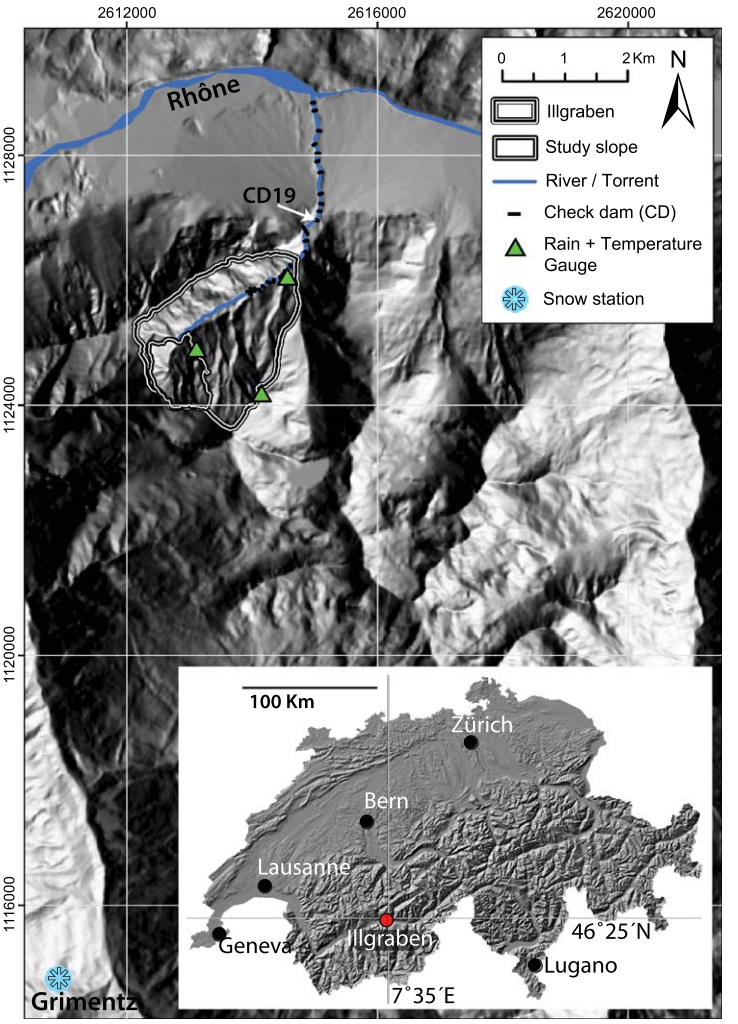

Figure 1. Location of the Illgraben in the Rhone Valley and Switzerland.

2. Slope Failures and Debris Flows in the Illgraben

The Illgraben is a small (4.6 km^2), NE facing catchment discharging into the Rhone Valley in southwest Switzerland (Figure 1), formed within highly fractured Triassic metasedimentary rocks, predominantly quartzites, limestones, and dolomites [*Gabus et al*., 2008]. It is of great research interest because of its large sediment output into the Rhone River of ~60,000–180,000 m^3 yr^{-1} mostly in the form of debris flows [*Berger et al*., 2011]. As a result, the Rhone River downstream of the Illgraben has developed a braided morphology over a reach more than 6 km in length.

Large debris flows have been measured at the bottom of the Illgraben fan since 2000 by the WSL. We utilize part of this record from 2000 to 2009, containing 36 debris flows with estimated volumes between 2900 and 107,000 m^3 [e.g., *McArdell et al*., 2007; *Schlunegger et al*., 2009; *Bennett*, 2013] to calibrate parts of our model. The largest documented event with a total volume of several hundred thousand cubic meters occurred on 6 June 1961, causing considerable damage on the debris flow fan. The sediment discharge regime is also characterized by floods and smaller debris flows (<3000 m^3), but these are minor contributions to the sediment budget. In 2007 when more detailed measurements were made, 16 of 19 events were floods contributing ~1600 m^3 of sediment, or 8% of the 20,000 m^3 of sediment transported by the three large debris flow events. Instrumentation is removed from the channel at the end of October and reinstalled at the beginning of May. Therefore, sediment discharge is only recorded from May to October.

Several studies have investigated the production and transfer of sediment through the Illgraben [e.g., *Bardou et al*., 2003; *Bardou and Delaloye*, 2004; *McArdell et al*., 2007; *Bardou and Jaboyedoff*, 2008; *Schlunegger*

et al., 2009; *Berger et al*., 2011; *Schürch et al*., 2011]. In a previous study, we used digital photogrammetry to produce a record of erosion and deposition in the upper catchment between 1963 and 2005 [*Bennett et al*., 2012, 2013]. More than 2000 landslides occurred between 1986 and 2005 from the most active slope in the catchment (our study area), spanning 6 orders or magnitude in volume and producing a mean erosion rate 0.39 ± 0.03 m yr^{-1} [*Bennett et al*., 2012]. The probability distribution of the landslides, with rollover below 233 m^3 and power-law tail above this volume, was attributed to two types of slope failure—shallow slumps and slides making up the rollover and deep-seated bedrock failures making up the power-law tail. The latter are the most significant for the sediment budget, accounting for more than 98% of the total sediment supply [*Bennett et al*., 2012]. We use this distribution to determine the volumes of slope failures in the sediment cascade model. Large slope failures are also documented earlier in the 20th century, in 1920, 1928, 1934, and 1961 [*Lichtenhahn*, 1971; *Gabus et al*., 2008]. The largest rock avalanche was on 26 March 1961 with a volume in the range of $3–5 \times 10^6$ m^3. The sediment generated by this event presumably led to the largest recorded debris flow later that year.

The controls on the hillslope erosion rate are ambiguous but a thermal control seems present. *Bennett et al*. [2013] showed that an increase in the mean rate of hillslope erosion in the 1980s in the Illgraben is most likely explained by the increased exposure of the hillslope to thermal weathering due to a significant reduction in snow cover in warmer periods. *Berger et al*. [2011] illustrated the occurrence of channel filling during the winter and spring seasons by slope failures between 2007 and 2009, supporting the hypothesis that thermal weathering could be the most important control on slope failure. We implement this potential thermal triggering of landslides in the model by conditioning landslide occurrence on the absence of snow cover, but we also experiment with other hypothetical triggering mechanisms and sediment input scenarios. Another important observation in the Illgraben is that hillslopes are eroding independently of channel incision and that a downstream-directed coupling is the dominant process in the catchment at this time scale [*Bennett et al*., 2013].

There are several possible triggering mechanisms of debris flows in the Illgraben channel system [*Bardou and Delaloye*, 2004; *Badoux et al*., 2009]. The largest debris flows, such as the one documented in 1961, are probably associated with failures of landslide dams [*Bardou et al*., 2003]. Debris flows may also result from hillslope landslides with additional entrainment along the channel [*Burtin et al*., 2012]. *Bardou and Dalaloye* [2004] argue for climatic triggers related to temperature, e.g., snowmelt runoff from avalanche deposits or frost cracking due to ground freezing. However, the most frequent mechanism of debris flow generation is thought to be by entrainment of sediment stored in the channel during runoff events that are predominantly generated by heavy summer rainstorms [*Badoux et al*., 2009; *Bennett et al*., 2013].

We therefore conceptualize debris flow triggering in the model by surface runoff and subsequent entrainment. Because snowmelt can play an important role in conditioning or even triggering debris flows in the late spring and early summer, our modeling approach includes the simulation of hydrological processes of precipitation, snow accumulation and melt, and evapotranspiration, which together determine runoff and the conditions for generating floods and debris flows.

3. Model Structure and Calibration

The sediment cascade model SedCas is a conceptual water and sediment transfer model that is spatially lumped at the basin scale (Figure 2). It consists of two parts: a hydrological and a sediment model. The hydrological model simulates the water balance for the basin including all relevant hydrological processes that lead to surface runoff generation. The sediment model simulates the cascade of sediment from landslides to hillslopes and into channels, and together with the runoff simulated by the hydrological model determines sediment discharge events in the form of sediment-poor floods, sediment-laden floods (or debris floods), and debris flows. The time step of both models is daily. The calibration of the SedCas model components for the Illgraben was performed as much as possible by independent estimation of model parameters and without fine tuning of the model output. All model parameters are summarized in Table 1.

The hydrological model is a lumped model based on the linear reservoir concept which is the basis for many conceptual watershed models [e.g., *Eriksson*, 1971; *Kirchner*, 2009]. The water storage reservoir is fed by rainfall and snowmelt and depleted by evapotranspiration and runoff. Daily precipitation is derived from the MeteoSwiss RhiresD gridded product as a mean depth over cells that cover the Illgraben basin. The

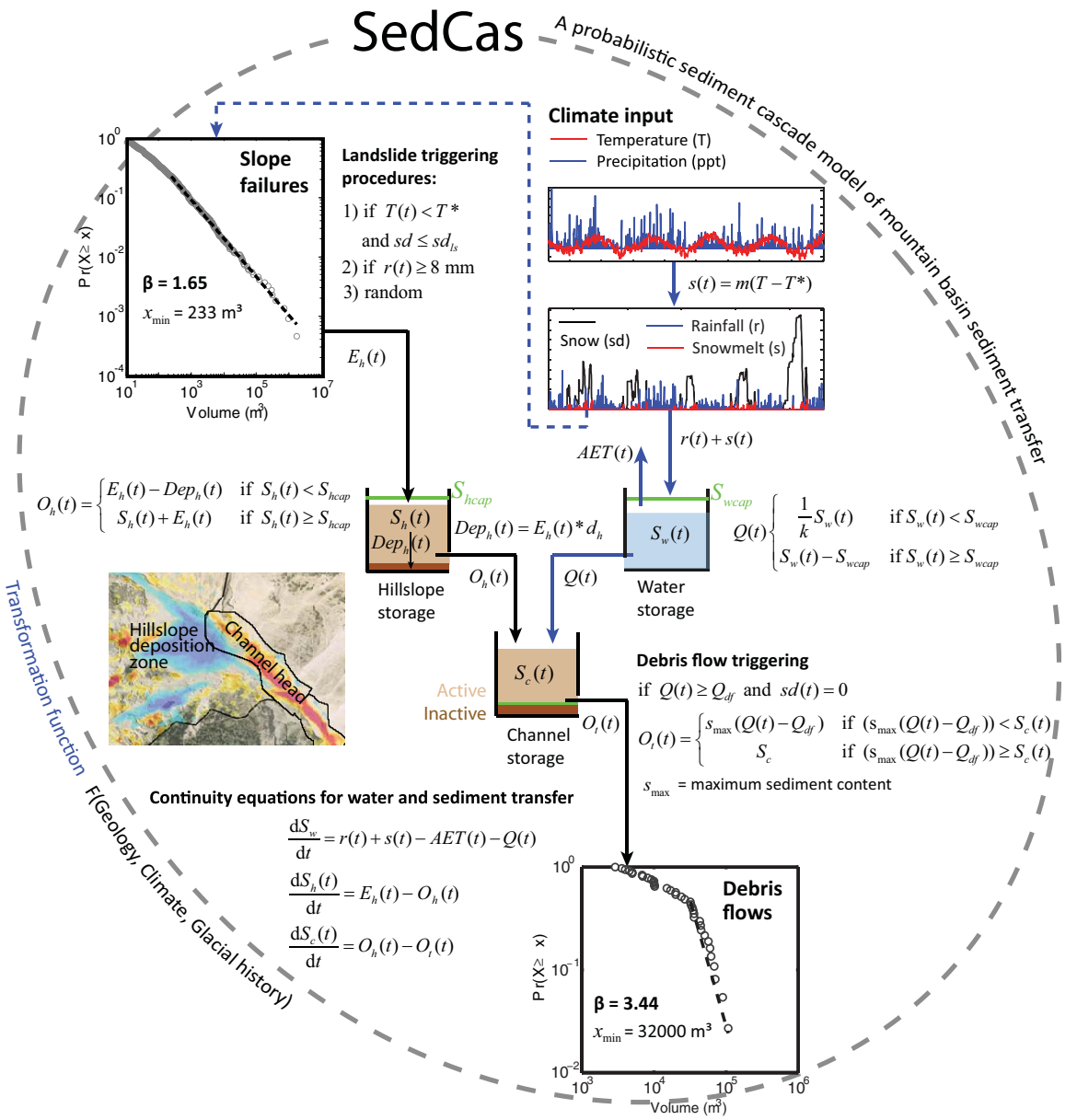

Figure 2. SedCas model structure. The probability distribution of slope failures is from *Bennett et al*. [2012]. The distribution of sediment discharge events (debris flows) are those measured at the catchment outlet from 2000 to 2009.

interpolation method in RhiresD follows that of *Frei and Schär* [1998]. The area-integrated precipitation estimates from RhiresD are more reliable than ground measurements in the Illgraben. Daily air temperature is measured at Sion, ~15 km SW of the Illgraben, and interpolated to mean basin altitude with a monthly lapse rate estimated from Illgraben station data [*Bennett et al*., 2013]. Daily solar radiation and cloud cover data are also measured at Sion. Precipitation is separated into solid and liquid phase by a temperature threshold and a degree-day model is used to estimate snowmelt. Details of the hydrological model and its calibration are in section 3.1.

The sediment model is a lumped model of the sediment transfer system and consists of two sediment storage reservoirs, one for the hillslope and the other for the channels. Sediment is supplied stochastically into the reservoirs by slope failures derived from a probability distribution of landslides on the hillslopes. In our application to the Illgraben, we consider the hillslopes at the head of the main debris flow channel to be our main sediment production area, as these have been shown to be the most active in the basin

Table 1. Model Parameters[a]

Parameter	Description	Value	
T^*	Threshold temperature for snow accumulation, melt, and melt of water frozen in the ground	0°C	
m	Snowpack melt rate factor	2.2 mm °C^{-1} d^{-1}	
δ_{sum}	Albedo (summer)	0.3	x
δ_{win}	Albedo (winter)	0.8	x
α	Parameter in the calculation of evaporation efficiency γ	0.2 mm^{-1}	
S_{wcap}	Basin-wide water storage capacity	21 mm	x
k	Residence time of water in the storage reservoir	2 days	
x_{min}	Minimum landslide volume from the power-law tail	233 m^3	x
β	Power law scaling exponent in landslide distribution	1.65	x
μ	Mean of the lognormal distribution of landslides $< x_{min}$	3.36 m^3	x
σ	Standard deviation of lognormal distribution of landslides $< x_{min}$	1.18 m^3	x
d_h	Hillslope redeposition rate	0.12	x
S_{hcap}	Hillslope storage volume threshold	7.5×10^4 m^3	x
sd_{ls}	Threshold snow depth for landslides triggered by thermal weathering (procedure 1; in SWE)	12 mm	x
r_{ls}	Threshold rainfall for landslides triggered by rainfall (procedure 2)	8 mm d^{-1}	x
Q_{df}	Critical discharge to generate a sediment discharge event	0.33 m^3 s^{-1}	x
s_{max}	Maximum potential ratio of sediment to water in the flow, which equates to a maximum sediment concentration of 0.39	0.65	x

[a]Parameters estimated independently are indicated with x.

[*Schlunegger et al*., 2009; *Berger et al*., 2011]. This area is marked as the study slope in Figure 1 and the probability distribution of landslides has been developed for it by *Bennett et al*. [2012]. The study area does not include downstream tributaries to the main channel which may produce occasional sediment input, but are generally much less active. The hillslope reservoir represents the storage of sediment at the base of the hillslopes in the study area into which a fraction of sediment from slope failures is temporarily deposited enroute to the channel reservoir (see Figure 2) [*Bennett et al*., 2013]. The channel reservoir represents the portion of the main debris flow channel between the base of the hillslopes in the study area and the fan apex (near to CD19 in Figure 1). See *Bennett et al*. [2013] for a schematic and further explanation of the sediment routing system. Details of the sediment model and its calibration are in section 3.2.

3.1. Hydrological Model

3.1.1. Snow

The hydrological model uses a simple description of snow accumulation and melt to predict snow depth at a point as a function of elevation, temperature, precipitation, and a constant melt factor [e.g., *Perona et al*., 2007; *Molini et al*., 2011]. Accumulation of the snowpack occurs through cumulated precipitation events when temperature is below a threshold T^*. On days when temperature exceeds T^* the snowpack melts at a rate proportional to temperature, $s(t) = m(T - T^*)$ where s is daily snowmelt and m is the melt-rate factor. Snowmelt feeds the water storage reservoir together with rainfall. The model may be driven by observations of daily precipitation and temperature or stochastic simulations thereof.

For the calibration of the snow module, we used snow depth data from the Grimentz station 6 km to the southwest of the Illgraben (Figure 1), chosen from several surrounding stations due to its similar elevation to the study area. We converted snow depth into snow-water equivalent (SWE) using a constant density 0.3 g cm^{-3}, which was an average of fresh and old snow measurements taken at the nearby Arolla glacier [*Carenzo et al*., 2009] assuming an equal contribution of old and new snow to the snowpack. We calibrated T^* and m based on the duration of snow cover and snow depth for the period 2000 to 2009. We found that having the same threshold temperature $T^* = 0$°C for accumulation and ablation and $m = 2.2$ mm °C^{-1} d^{-1} produced the best results (RMSE = 1.5 mm d^{-1}). Figure 3a shows an example of the time series of modeled snow depth compared to the observed snow depth at Grimentz (in SWE), along with modeled snowmelt and rainfall. The assumption of a constant snow density does not allow the degree-day model to capture the fluctuations in SWE accurately; however, the duration of snow cover, which is the key component for us, is represented reasonably well together with the probability distribution of snow depth (Figure 3b). A more complex snow accumulation and melt model would be needed in spatially distributed applications.

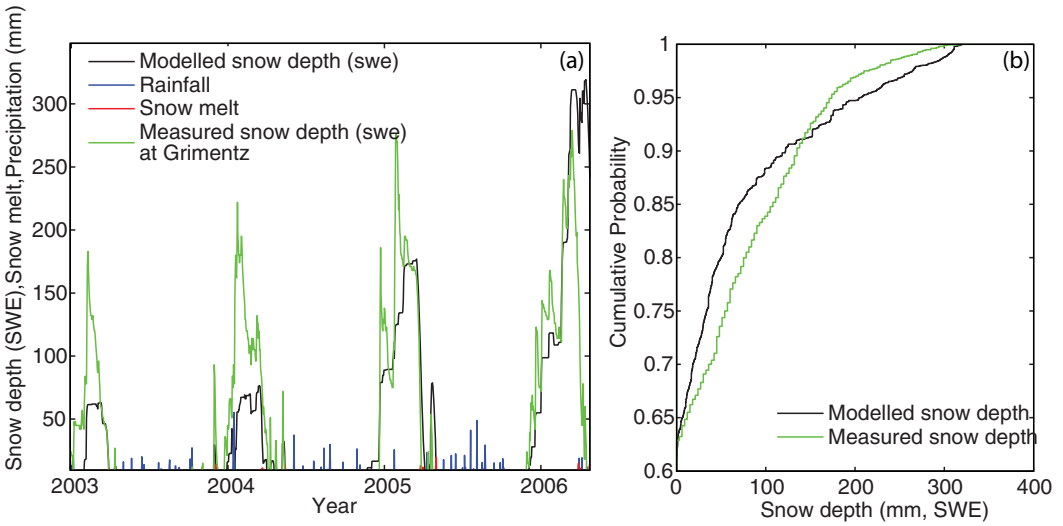

Figure 3. (a) Example of time series of modeled daily snow depth, rainfall, snowmelt, and measured snow depth (in SWE) at Grimentz. (b) Cumulative distribution of modeled and measured daily snow depth for the period 2000–2009.

3.1.2. Water Balance

The water balance in the hydrological model is solved with a linear reservoir model at the daily time scale. The water storage reservoir represents the capacity of the soil (weathered bedrock) in the basin to store and discharge water. It is fed by snowmelt and rainfall and depleted by evapotranspiration and runoff:

$$\frac{dS_w}{dt} = r(t) + s(t) - AET(t) - Q(t) \tag{1}$$

where S_w is water storage in the reservoir, r is rainfall, s is snowmelt, AET is evapotranspiration, and Q is runoff. All of these are daily basin-averaged values in millimeters.

Actual evapotranspiration is modeled as a fraction of daily potential evapotranspiration (PET) which is computed with the Priestley-Taylor method [*Priestley and Taylor*, 1972]. This requires time series of mean daily temperature, solar radiation, cloud cover, and values for albedo and elevation. We obtained the time series from the MeteoSwiss weather station in Sion and used the mean elevation of the study site as the representative point. Albedo was $\delta_{\text{sum}} = 0.3$ for the summer and $\delta_{\text{win}} = 0.8$ for the winter, which are average values for bare ground and snow, respectively. AET is computed as a fraction of PET,

$$AET = \gamma PET \tag{2}$$

where γ is an efficiency parameter which is determined as a function of catchment water storage following *Tuttle and Salvucci* [2012],

$$\gamma = \left[1 - e^{(-\alpha S_w)}\right] \tag{3}$$

where α is a parameter that determines how water availability in the subsurface limits evapotranspiration at the potential rate. The parameter $\alpha = 0.2$ mm^{-1} was calibrated to reproduce the mean annual AET for the study region [*Hydrological Atlas of Switzerland*].

Runoff from the water storage reservoir takes place under two conditions. When the water storage capacity S_{wcap} is not reached, outflow is computed as a function of the stored amount assuming a linear reservoir relation. When the capacity is exceeded, then all excess water generated by rain and/or snowmelt is discharged into the channel system and out of the basin:

$$Q(t)\begin{cases} \frac{1}{k} S_w(t) & \text{if } S_w(t) < S_{wcap} \\ S_w(t) - S_{wcap} & \text{if } S_w(t) \geq S_{wcap} \end{cases} \tag{4}$$

The residence time k represents the attenuation of runoff through subsurface flow paths. Based on our observations in the Illgraben, we allow runoff from the subsurface reservoir only when $T > T^*$. During the

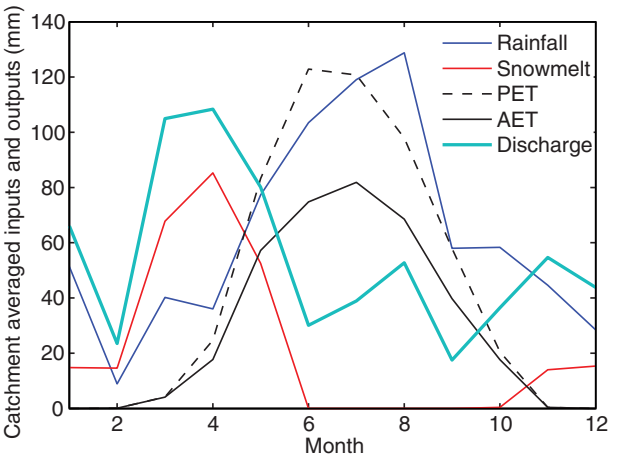

Figure 4. Seasonal distribution of modeled hydrological variables. Plotted are the monthly means over the simulation period 2000–2009.

winter months, water in the subsurface reservoir stored in bedrock fractures, coarse sediment deposits and soil is assumed to be frozen. Only when the temperature rises above T^* draining of water is initiated. We made a best guess of $k = 2$ days based on observations of discharge in the channel in days following rainfall; however, we note that the model results, including debris flow timing, are not very sensitive to k. The water storage capacity S_{wcap} was independently estimated from the difference in observed runoff and basin-integrated rainfall for several flood and debris flow events in the catchment in 2005 and 2006 [*Nydegger*, 2008]. For rainfall events without snowmelt we argue that the maximum observed difference represents the catchment storage capacity. Averaged over the catchment this results in $S_{wcap} = 21$ mm. This is a low estimate because it is based on only 2 years of data and assumes water storage was empty at the beginning of the events. In the calibration of the model, we investigated the effect of larger values as well.

Figure 4 shows the seasonal distributions of modeled hydrological variables for the period 2000–2009. Rainfall is maximum during the summer months, but *AET* removes a large fraction of the water during this time, reducing discharge. Discharge is highest in the spring as a result of large inputs of snowmelt and low values of *AET*. Mean annual values of rainfall, *AET*, and discharge after calibration are 1018, 362, and 657 mm, respectively. These agree with values reported for the region in the Hydrological Atlas of Switzerland and a recent study by *Fatichi et al*. [2013]. We have no other means of calibrating the hydrological outputs in more detail without continuous discharge measurements at the catchment outlet.

3.2. Sediment Model

3.2.1. Sediment Supply by Slope Failure

Sediment is delivered into the hillslope storage reservoir by slope failures at an average annual hillslope erosion rate equal to the observed rate $\overline{E_h} = 0.39$ m yr^{-1} [*Bennett et al*., 2012]. We experimented with five scenarios/procedures of sediment input into the model. The first three procedures are stochastic and slope failures are drawn from the probability distribution determined from observations by *Bennett et al*. [2012], while the remaining two procedures are hypothetical deterministic reference cases.

Procedure (1) simulates triggering related to freezing. Large failures are triggered on days with air temperature $T \leq 0$°C and snow depth $sd < sd_{ls}$. This procedure is based on the argument that freezing conditions without an insulating layer of snow on the ground are conducive to thermal weathering and slope failure [*Bardou and Delaloye*, 2004; *Bennett et al*., 2013]. The limiting snow depth $sd_{ls} = 12$ mm (SWE) was calibrated to reproduce the observed mean annual number of large failures ($n = 25$) and the average annual erosion rate $\overline{E_h}$. The calibrated snow depth corresponds to about 40–80 mm of snow on the ground which is less than what is normally required to insulate the ground from air temperature variations [e.g., *Keller and Gubler*, 1993; *Rödder and Kneisel*, 2012].

Procedure (2) simulates triggering related to rainfall. Large failures are triggered by daily rainfall $r > r_{ls}$. The critical rainfall threshold $r_{ls} = 8$ mm d^{-1} was calibrated to reproduce the observed mean annual number of large failures n and the average annual erosion rate $\overline{E_h}$.

Procedure (3) simulates a random triggering of slope failure. In this procedure, n large failures are generated from the probability distribution of *Bennett et al*. [2012] independently in time, without any relation to climatic forcing.

The commonalities between procedures (1–3) are that in addition to the large slope failures we also always generate a background erosion rate by small landslides from a lognormal probability distribution, which we fitted to the observed small failures ($x < x_{min}$) with a mean $\mu = 3.36$ m^3 and standard deviation $\sigma = 1.18$ m^3, i.e., the rollover region in *Bennett et al*. [2012]. Furthermore, for the large slope failures, we imposed an upper failure volume of 3×10^6 m^3, which is the volume of the largest known landslide in the catchment in 1961 [*Gabus et al*., 2008] because we know that a larger event did not occur in the study period. For each procedure, we generate 1000 realizations, each 10 years long, representing the 2000–2009 period. Because of the random selection of slope failure volumes, the annual erosion rate of each simulation run is variable. However, the average annual erosion rate of 1000 runs used in the simulation is equal to the observed mean $\overline{E_h}$.

These triggering procedures are also compared with two reference procedures that do not utilize the observed probability distribution of slope failures but which also preserve $\overline{E_h}$. Procedure (4) mimics the case of a large rockfall filling the hillslope and channel storage at the beginning of the simulation period. The volume of sediment entered into the channel reservoir corresponds to 10 years' worth of sediment (3×10^6 m^3) in a single failure. Procedure (5) represents a constant daily sediment supply of 800 m^3 d^{-1} by slope failures into the channel system and ignores day-to-day variability. These are hypothetical scenarios that are expected to give unrealistic results.

3.2.2. Sediment Storage Accounting

The sediment cascade model consists of two sediment reservoirs representing hillslopes and channels. Volumetric continuity is ensured in each of the reservoirs:

$$\begin{aligned} \frac{dS_h(t)}{dt} &= E_h(t) - O_h(t) \\ \frac{dS_c(t)}{dt} &= O_h(t) - O_t(t) \end{aligned} \tag{5}$$

where S_h(t) is the hillslope storage volume, E_h(t) is hillslope erosion rate by slope failure, O_h(t) is hillslope sediment output, S_c(t) is channel storage, and O_t(t) is catchment output by sediment discharge events.

The hillslope reservoir serves as temporary storage, where a part of the sediment generated by hillslope landslides is deposited, accounting for the fact that not all sediment generated by landslides passes directly into the channel system. The deposition rate is a constant fraction of eroded sediment on a given day $Dep_h(t) = d_h E_h(t)$. The hillslope redeposition parameter $d_h = 0.12$ was estimated from the observed storage on hillslopes and erosion estimated by digital elevation model (DEM) differencing [*Bennett et al*., 2012, 2013]. We impose a critical storage S_{hcap} above which the hillslope reservoir cannot store sediment anymore and releases it into the channel in a single landslide. This threshold represents the condition when the hillslope debris fans have reached a critical friction angle at which they fail. S_{hcap} was estimated as the maximum observed hillslope deposition in the analysis period of *Bennett et al*. [2012, 2013]. The hillslope sediment output into the channel reservoir is then:

$$O_h(t) \begin{cases} (1-d_h)E_h(t) & \text{if } S_h(t) < S_{hcap} \\ S_h(t) + E_h(t) & \text{if } S_h(t) \geq S_{hcap} \end{cases} \tag{6}$$

The initial condition for the hillslope storage reservoir $S_h(0) = 2.5 \times 10^4$ m^3 was estimated from the time series of DEMs described in *Bennett et al*. [2013].

The channel reservoir receives sediment from the hillslopes and releases it periodically in the form of debris flows and floods. It is conceptualized to consist of two components: active and inactive storage (Figure 2). This conceptualization reflects different residence times and an inaccessibility of sediment for mobilization, e.g., in floodplains [*Nakamura and Kikuchi*, 1996] or base of debris flow deposits [*Lancaster and Casebeer*, 2007]. In the case of the Illgraben, however, this stratification of storage in the channel is necessary also because of human intervention. Inactive storage here represents the sediment stored behind a series of

check dams along the channel above the fan apex (Figure 1). Inactive storage is treated as inaccessible to debris flows and was estimated to be 3×10^6 m^3 from the 1963 DEM and an earlier topographic map. The active channel storage S_c(t) is any sediment stored above this amount. It is a key component of the SedCas model because the actual sediment discharge is dependent on the availability of sediment in active storage at the time of the event.

The initial condition for the active channel storage for each model run $S_c(0)$ is set to almost empty based on our data which show that the channel was eroded to its lowest level in almost 50 years in 1998, only 2 years before the start of the calibration period [see *Bennett et al*., 2013, Figure 7]. We also observed that there were only relatively few and small debris flows in 2000 and 2001, which we interpret as further evidence of a lack of sediment in the channel at this time or temporary blocking of efficient sediment transfer through the system by older debris flow deposits.

3.2.3. Debris Flow Generation

Sediment discharge events are generated in the model by hydrological forcing, i.e., by runoff in the channel system (Figure 2). When the water storage capacity S_{wcap} is reached, any excess snowmelt or rainfall generates surface runoff Q(t) according to equation (4). For triggering large sediment discharge events, we introduce the critical discharge Q_{df}, which is a discharge that corresponds to a critical bed shear stress needed to generate an event, shear stress being a function of discharge for a given channel geometry. When Q_{df} is exceeded, the excess discharge is able to entrain and transport sediment at a rate specified by $s_{\max}$ and sediment availability. These events are in fact a spectrum of sediment discharge events ranging from floods to debris flows limited and unlimited by sediment supply. The sediment discharge rate O(t) is computed as:

$$O(t)\begin{cases}\frac{\rho_{df}}{\rho_h} s_{\max}\left[Q(t)-Q_{df}\right] & \text{if } \frac{\rho_{df}}{\rho_h} s_{\max}\left[Q(t)-Q_{df}\right] < S_c(t) \\ S_c(t) & \text{if } \frac{\rho_{df}}{\rho_h} s_{\max}\left[Q(t)-Q_{df}\right] \geq S_c(t)\end{cases} \tag{7}$$

where ρ_{df} is the dry bulk density of debris flows, ρ_h is the dry bulk density of hillslope sediment stored in the channel, and $s_{\max}$ is a maximum ratio of sediment to water in a discharge event unlimited by sediment supply. Because we do not have enough information about the differences in bulk densities of hillslope and channel deposits, we assume that the porosity of the sediment is identical on hillslopes, in channels and debris flows, and assume that $\rho_h = \rho_{df} = 1800$ kg m^{-3}, which is the mean debris flow density estimated from observations at the force plate described by *McArdell et al*. [2007]. However, different bulk densities of hillslope and debris flow material may be accounted for in the model in equation (7) if such data are available. In our model, we hypothesize that flows below Q_{df} transport fine sediment in suspension, however, they do not qualify as large sediment discharge events, and contribute insignificantly to the total sediment budget.

Similarly to the treatment of the water reservoir, we assume that the channel reservoir output is reduced in the winter because of snow accumulation in the channel system and increased sediment cohesion due to frost. Although the debris flow monitoring system is turned off in the winter, from occasional on-site observations we know that runoff and sediment discharging events, including debris flows, are rare. We therefore include an additional condition for debris flow generation in the model that is the absence of snow cover. This is based on the hypothesis that snow accumulations in the channel block debris flows as has been suggested for the Illgraben [*Bardou and Delaloye*, 2004] and for the Ritigraben [*Stoffel et al*., 2008]. In other systems, this requirement may be removed.

We also tested other debris flow generation procedures. For example, debris flows were triggered when discharge Q exceeded Q_{df}, but in contrast to equation (7), the generated debris flow had a potential size $\frac{\rho_{df}}{\rho_h} s_{max}[Q]$, i.e., all discharge was able to entrain sediment, not just discharge above Q_{df}. Another tested option was to bypass the hydrological model, assume that $Q = P$ and trigger debris flows when precipitation exceeded Q_{df} on days when $T > 0$°C. A generated debris flow then had a potential size $\frac{\rho_{df}}{\rho_h} s_{max}[P]$. The effects of these triggering procedures on the probability distribution of generated debris flows are compared.

3.2.4. Model Calibration

The majority of the SedCas model parameters were estimated from independent observations of hillslope and channel processes, and from hydrological considerations. As explained earlier, for the hydrological

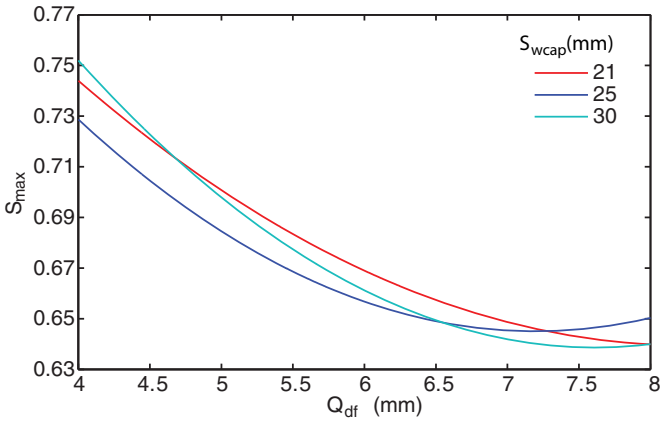

Figure 5. Combinations of Q_{df} and s_{max} leading to a simulated mean debris flow volume equal to that observed (30.4×10^3 m^3) for three different S_{wcap} values.

parameters we required a fit to snow cover data and correct representation of the mean annual and seasonal hydrological regime. For the sediment parameters, we required that the model reproduces basis statistics such as the mean number of slope failures and the mean erosion rate accurately. The most sensitive parameters were the threshold parameter for debris flow generation Q_{df} and the maximum ratio of sediment to water in a discharge event unlimited by sediment supply s_{max}.

The joint calibration of Q_{df} and s_{max} was conducted by finding combinations of these parameters that result in the mean observed debris flow volume for a range of realistic water storage capacities S_{wcap} (Figure 5), showing that mean debris flow volume is sensitive to Q_{df} and s_{max} but not to S_{wcap}. In order to constrain the values of Q_{df} and s_{max} further, we made a selection of the observed debris flows considered to be transport limited, i.e., with maximum sediment concentration, and calculated the mean s_{max} for different Q_{df} values using the observed rainfall totals on days of debris flows. In this calculation, we assume that all basin-wide rainfall is converted into discharge, which is a reasonable assumption for days with intense rainfall. The combination of these two approaches gives $Q_{df} = 6.2$ mm d^{-1} (equivalent to a discharge rate of 0.33 m^3 s^{-1}) and $s_{max} = 0.65$, resulting in a maximum volumetric sediment concentration in transport-limited events $c_{max} = 0.39$. This is a maximum possible concentration in the model, because the actual sediment concentration of a discharge event is dependent on sediment availability in channel storage and may be much less than c_{max}. The final list of all parameters is provided in Table 1.

In order to compare the different hillslope landslide generating procedures and their realism, we used the mean sediment residence time in the channel reservoir and debris flow statistics. The observed mean residence time was estimated from data based on DEM analyses [*Bennett et al*., 2012, 2013] as the volume of the channel reservoir, i.e., sediment storage, divided by the flux through it [*Eriksson*, 1971], assuming that all sediment in the reservoir has an equal probability of evacuation [e.g., *Benda and Dunne*, 1997; *Lisle and Church*, 2002; *Malmon et al*., 2003]. We calculated sediment storage for each period (1986–1992; 1992–1998; and 1998–2005) above the 1998 channel surface, the lowest of the DEMs, and calculated the flux through the channel as the sum of the input from the hillslopes and channel storage change for that period. We obtained an average sediment residence time of 450 days, which is in general agreement with a residence time of 1 year estimated by *Berger et al*. [2011]. This value was then compared with simulations with different sediment input scenarios.

4. Results

We first address the main question—is our simple conceptual sediment cascade model able to explain the transformation of the probability distribution of slope failures into that of debris flows in terms of the stochastic triggering and sediment transport mechanisms in the basin? We then show how the available sediment storage determines the division of events into transport and supply-limited cases. Finally, we present results that show that in our approach debris flows may be generated for a wide range of rainfall intensities, in agreement with observations, which may help explain the limitations of a single rainfall intensity threshold for debris flow initiation.

4.1. Probability Distribution of Debris Flows

The observed and simulated probability distributions of debris flows for the 10 year period 2000–2009 are shown for landslide triggering procedure (1) in Figure 6. Because the Illgraben monitoring system is

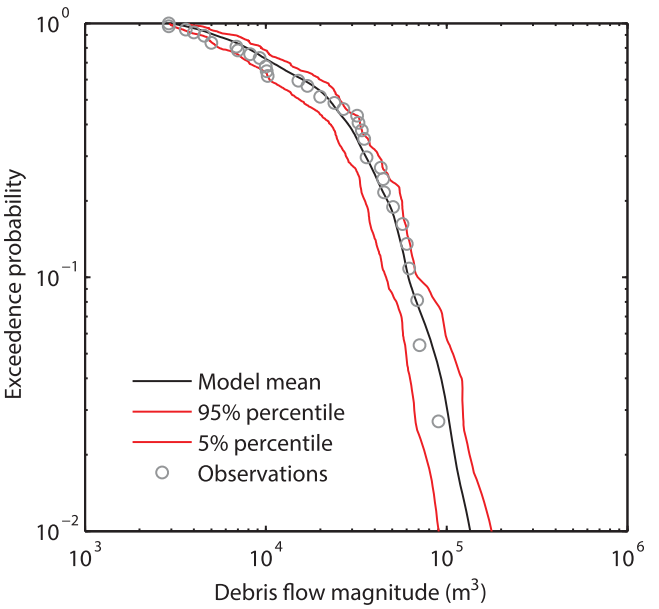

Figure 6. Exceedence probability distribution of modeled and observed debris flows based on model runs with sediment input procedure (1). This procedure generates large failures on days with air temperature $T \leq 0°C$ and snow depth $sd < sd_{ls}$, while small failures occur at random. The black line is the mean of 1000 realizations and the red lines are the 5% and 95% percentiles.

designed to only record data for relatively large debris flows [*Badoux et al.*, 2009] only these events are shown in Figure 6. The result shows a close fit to the observed probability distribution of debris flows, even though the model was not explicitly fine tuned to achieve this. Practically all observations are contained within the 90% confidence bounds of the simulations.

Our first aim was to investigate the conditions that lead to the transformation of the probability distribution of slope failures into that of debris flows and our results show the following. The general shape of the distribution of debris flow volumes with a sharp dropoff and steep tail is indeed very different from the distribution of the input landslide volumes, which has a less steep and much more consistent power law behavior over a much greater range typical of landslide distributions, see also schematic in Figure 2 or data in *Bennett et al.* [2012]. A similarly shaped distribution of debris flows was also found by *Bardou and Jaboyedoff* [2008] for historical debris flows in Switzerland. This raises the question of what is controlling the shape of the debris flow distribution. A comparison of debris flow distributions generated by different triggering procedures (Figure 7) shows that it is fundamentally the threshold discharge Q_{df} that, through its role in limiting the volume of discharge Q capable of entraining sediment, best explains the overall shape of the distribution of debris flows. The other triggering procedures overestimate debris flow volumes. The distributions of large events for the triggering procedures with Q and P are almost identical, which is due to the fact that these largest debris flows occur under heavy rainfall when the soil water storage is at capacity S_{wcap} and all precipitation is transferred directly into runoff. Although the hydrological model component may not play a key role for the size of these largest events, it does affect their timing, as shall be shown in section 4.3.

A secondary control on the shape of the debris flow distribution is the sediment-supply limiting condition, which decreases the size of some of the potential debris flows (hypothetical supply unlimited), particularly of the largest events, and thus steepens the tail of the distribution (Figure 7). This is the case for all triggering procedures and explains their similar tails. We study sediment supply limitation of events in more detail in section 4.2.

We found that the stochastic landslide sediment input scenarios result in very similar results and all would fit the observed debris flow data reasonably well. The dropoff point x_{min}, the slope of the power-law tail β, and mean number and volume of debris flows for all procedures are listed in Table 2 for simulated and observed data. The overestimation of large debris flows by all procedures is not a concern, and is mainly due to the fact that we simulate the production of events in the study area in the upper basin and do not consider the redeposition or stopping of debris flows on the debris flow fan itself before they reach the gauging station. Measurements between the fax apex and toe by *Schürch et al.* [2011] have shown that this affected about 35% of debris flows events, mostly small ones. In many aspects, the completely random slope failure generation procedure (3) performed equally well or even better than the more physically based procedures connected to climatic conditioning (freezing and rainfall). On the basis of the results in Table 2, it is indeed very difficult to objectively judge which of the three procedures is best. This means that

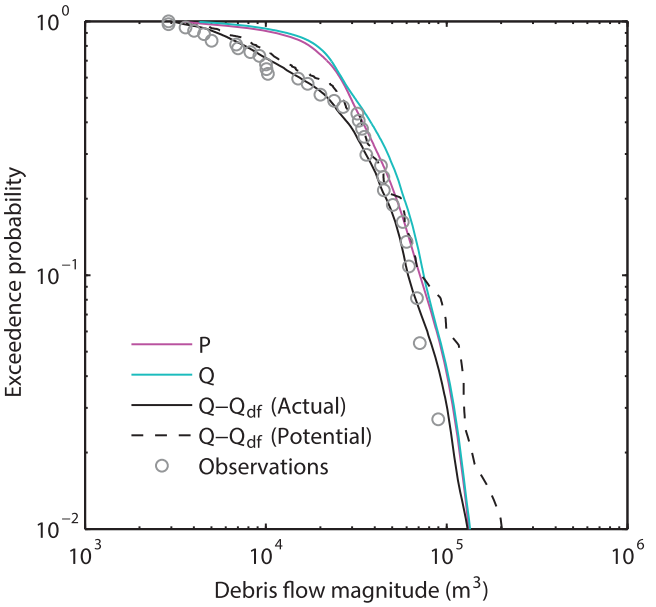

Figure 7. Exceedence probability distributions of observed and modeled debris flows for three different triggering procedures, *P*, *Q*, and $Q - Q_{df}$. In each case, debris flows are triggered on days where Q_{df} is exceeded but the generation of debris flow volumes by *P* and *Q* does not involve Q_{df}. See text for details. The potential distribution of debris flows for the case of unlimited sediment supply is also shown for comparison with the actual modeled distribution of debris flows generated by $Q - Q_{df}$.

the sediment cascade, the runoff regime and debris flow generation, filter out many of the differences in the sediment input procedures to the point that they are not evident in the sediment discharge output anymore. In contrast, the two hypothetical reference procedures do in fact significantly depart from the observed debris flow statistics. For example, the initial large sediment supply (procedure 4) produces too many supply prohibited events as the sediment in storage is exhausted in time, and the constant daily supply of sediment (procedure 5) leads to an overestimation of the number of debris flows, an underestimation of their average volume, and as a result a mean residence time of sediment in the channel that is much smaller than that observed.

4.2. Transport and Sediment Supply Limitations

To investigate the detailed impact of sediment storage on simulated sediment discharge events at the event scale, we first looked at the reduction of the simulated event volumes from their potential size in the model. This is shown in Figure 8 where the mean simulated event volumes are plotted against their potential volumes for the sediment input procedure (1). There is clearly a large variability in simulated event volumes as a function of the availability of sediment. While small events tend not to be limited by sediment availability, the large ones definitely are. Overall, sediment supply limited 29–42% of the debris flows in the first three sediment input procedures, and in fact in 11–25% cases the lack of sediment completely prohibited a sediment discharge event from occurring in the model (Table 2). Of course we cannot verify these results with data, but

Table 2. Results of 1000 Model Runs for Different Sediment Input Procedures Compared to Observations[a]

		Sediment Input From Probability Distribution (1000 runs)			Reference Procedures		
Measure	Observations	(1)[b]	(2)[c]	(3)[d]	(4)[e]	(5)[f]	(6)[g]
Mean number of dfs (>2900 m^3)	36	79*	86	78*	76*	110	77*
Mean df volume (10^3 m^3)	30.4	29.9*	24.5	25.6	35.3	22.3	36.8
Mean β of df distribution	3.44	3.8	3.2*	3.6*	3.1	3.7	3.6
Mean x_{min} of df distribution (10^3 m^3)	32.0	40.3	29.5	32.8*	32.1*	30.4	36.0
Mean residence time distribution (days)	450	641	382	422*	893	140	108
Mean % supply limited events		7	16	12	1	26	5
Mean % supply prohibited events		39	38	44	46	21	80
Mean % supply limited events (all)		30	42	29	1	33	54
Mean % supply prohibited events (all)		14	11	25	48	10	31

[a]df = debris flow; asterisks indicate the procedures that were closest to the observation for each measure. More debris flows may be simulated at the fan apex than are measured at the bottom of the fan. The percentage of supply-limited events is calculated as the % of potential events with lower than maximum sediment concentration. The percentage of supply-prohibited events is calculated as the percentage of potential events that did not occur due to the absence of sediment in the channel. The statistics are given for all events regardless of size.
[b]Large landslides are generated on days with air temperature $T \leq 0$°C and snow depth <12 mm SWE.
[c]Large landslides triggered by rainfall events >8 mm/d.
[d]Large landslides drawn randomly from power law.
[e]Single 3×10^6 m^3 rock avalanche at the beginning of the time series.
[f]Constant daily sediment supply (800 m^3 d^{-1}).
[g]Large landslides triggered by (1); debris flows triggered directly by rainfall instead of discharge from the hydrological model.

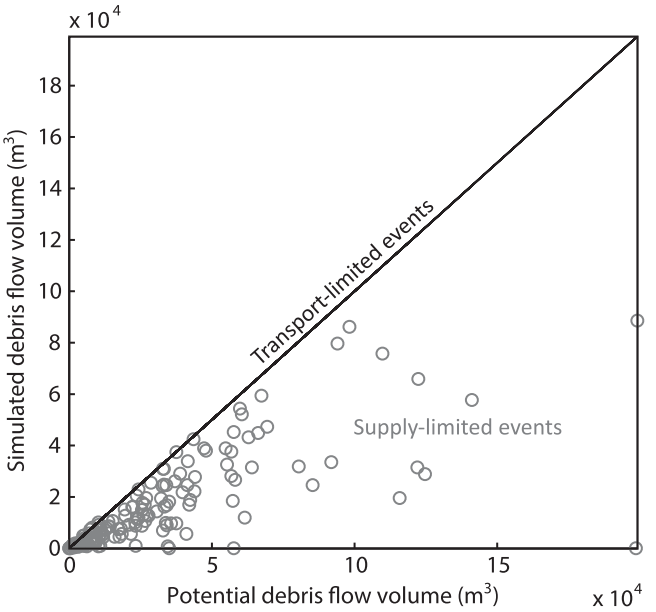

Figure 8. Mean simulated debris flow volumes of 1000 realizations versus potential debris flows. The black line is the one-to-one relationship in the case of an abundant sediment supply, i.e., represents transport-limited events. The model was run with sediment input procedure (1) and the event data are binned to compute the mean.

they do indicate that sediment supply is likely to be a key ingredient in debris flow formation even in this erosive catchment.

To explore the connection between runoff and sediment supply limitations in more detail, it is helpful to look at the results for sediment discharge $O(t)$ for all events. The runoff regime in our model determines the timing and magnitude of sediment discharge. Figure 9 shows the relationship between simulated water and sediment discharge in the model according to equation (7) for all events. We arbitrarily chose a volumetric sediment concentration $c = 0.05$ to distinguish between floods and debris flows because this is the lowest sediment concentration that was observed in our debris flow data set. We further subdivide floods into debris floods and floods with sediment concentration $c < 0.02$. The monitoring system in the Illgraben measures large events greater than 2900 m^3, which in our model consist mostly of simulated debris flows and some debris floods. However, it is also evident that the model also generates many lower sediment concentration floods, as we would expect in systems where supply limitations exist. As a result the model generates large variability in sediment transport for a given discharge, which is also often seen in sediment rating curves from observations.

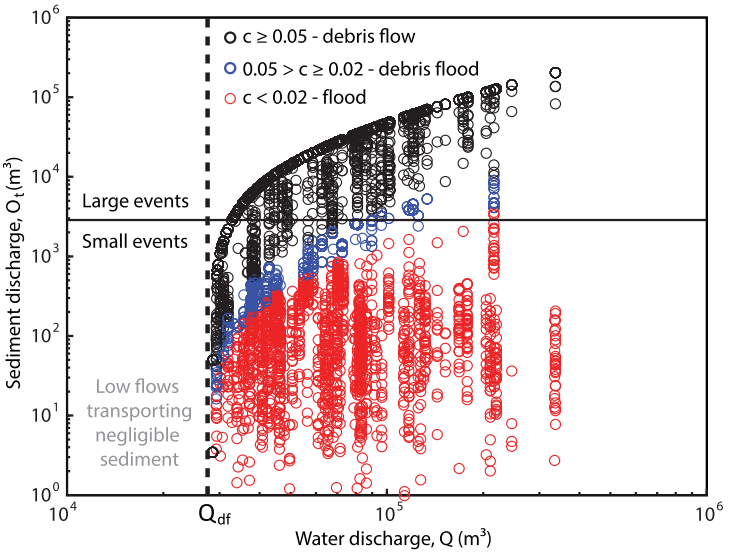

Figure 9. Relationship between sediment discharge and water discharge according to equation (7). Sediment concentration c is calculated as the volume of sediment in the total volume of water and sediment in an event, and where water is the excess discharge $Q - Q_{df}$. The Illgraben monitoring system only records large events (horizontal line in figure), which exceed a sediment discharge of 2900 m^3.

A consequence of sediment supply limitations is that the actual sediment concentration of individual sediment discharge events varies. The simulated cumulative probability distribution function of event sediment concentrations for the sediment input procedure (1), where concentrations may reach $c_{max} = 0.39$, is shown in Figure 10. The simulated mean sediment concentration of over 1000 runs for sediment input procedure (1) was about $c = 0.13$. The figure illustrates the full range of supply prohibited and limited conditions, as well as the dominating transport limited events. The distributions for the other three realistic sediment input procedures were similar with different proportions of the limiting cases.

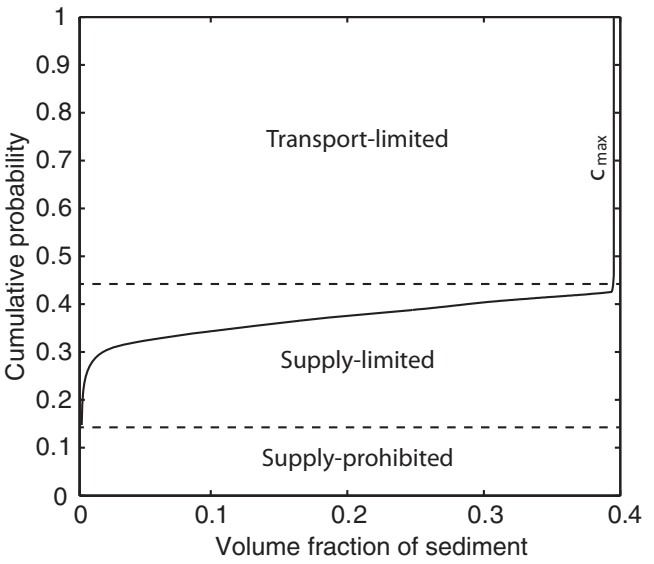

Figure 10. Cumulative probability distribution of the actual volumetric sediment concentration *c* of all modeled sediment discharge events, shown for procedure (1).

4.3. Relation of Debris Flows to Rainfall

Although the model is not designed to predict the actual timing of observed debris flows, we can expect that it reproduces the seasonality in sediment discharge insofar as it is driven by hydrological processes. Indeed, the main debris flow season between May and October is captured very well by SedCas with a peak in June (Figure 11a). Although the monthly mean runoff is highest between March and May (Figure 4), most of this occurs at low discharge rates through the process of snowmelt, and therefore, there are relatively few runoff events that exceed Q_{df} in that period. Additionally, snow cover during the spring inhibits many potential debris flows. The majority of runoff events that exceed Q_{df} and generate debris flows occur in response to heavy rainfall in the summer. The model also predicts some sediment discharge in other months of the year, apart from February when a permanent snow cover inhibits sediment discharge events altogether. We cannot verify this because data are not collected in these months. The model also generates an accumulation of sediment in the channel during the winter and spring by hillslope failures, which is then evacuated during the summer and autumn by debris flows (Figure 11b), in agreement with the observations of *Berger et al.* [2011].

Precise daily timing of debris flows is impossible to achieve due to the stochastic nature of sediment input into the channels and the area-averaged daily precipitation input in particular. However, we did conduct a comparison of the timing of modeled runoff events exceeding Q_{df} with observed debris flows, and found an agreement of about 30%, which increased to >50% if we consider a window of 3 days around the

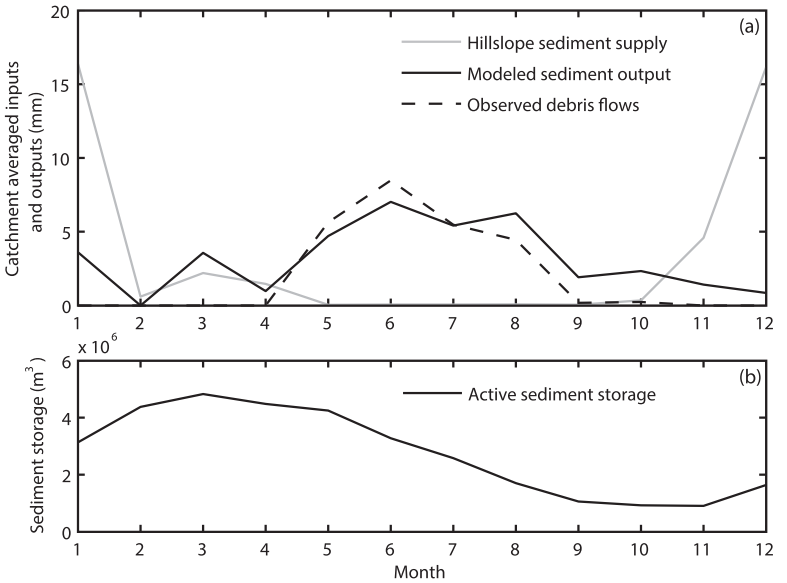

Figure 11. (a) Seasonal distribution of mean sediment input and output in (mm) modeled and observed; and (b) active sediment storage in (m^3), both shown for procedure (1).

observed debris flow. We know that high discharge and debris flows in the Illgraben may be generated by high-intensity summer storms of with durations much shorter than 1 day [*Badoux et al*., 2009].

However, even at the daily time scale we may investigate the relation of debris flows to rainfall, and use this as an additional verification of the SedCas model. In fact, the model captures very well the distribution of daily rainfall on days with observed debris flows (Figure 12a). This is not a trivial result because it has not been imposed in the calibration. It shows that debris flows may be generated on days with no rainfall (purely snowmelt) or with little rainfall falling on a wet basin, in conjunction with reality, with the right probability. We tested the effect of the rainfall-runoff process on this result by bypassing the hydrological model in the simulations and simply generating runoff equal to rainfall, ignoring the snow processes, soil water storage, evapotranspiration, etc. The distribution of daily rainfall on days with debris flows in this case was very different from that observed (Figure 12b). There is an underprediction of debris flows at low rainfall intensities and an overprediction at moderate rainfall depths. The rainfall debris flow triggering procedure (6) also dramatically overestimates the total number of debris flows as can be seen together with other statistics for sediment discharge events in Table 2.

5. Discussion

We present a sediment transfer model based on the sediment cascade concept with the overall aim of modeling and explaining the nonlinearity and stochasticity of sediment discharge from a mountain basin. Despite simplification and conceptualization, the processes and interactions of water and sediment production combine to produce complex and realistic behavior and result in highly nonlinear and stochastic sediment discharge. The model successfully reproduces the first-order properties of the sediment transfer system. In particular, the probability distribution function of debris flows and their seasonality, as well as sediment residence time in the channel in the Illgraben were well reproduced over the studied 10 year period. This is despite the fact that most parameters were independently estimated and not fine tuned to best reproduce the debris flow data. Within our conceptual sediment cascade framework we have necessarily neglected many processes and made several simplifications of the sediment production and transport processes in the Illgraben. We discuss here the main results in the context of the limitations of the modeling approach.

One of the key limitations of our model is the spatial averaging at the basin scale. The spatial averaging in our model does not allow us to include various processes, for example differential snowmelt on hillslopes, gullies, and channels, snow redistribution due to avalanches, that are important because they may both reduce debris flows for example by protecting the surface from erosion, or increase debris flows due to higher base flow and a sliding surface [*Bardou and Delaloye*, 2004]. Furthermore, the spatial integration and conceptualization of the sediment transfer system into hillslope and channel reservoirs does not allow us to study the detailed pathways of sediment between the multitudes of landforms that exist on a basin scale [e.g., *Theler et al*., 2010]. In the Illgraben application itself, we assumed that all of the sediment was produced by landslides in the active slopes in the upper watershed. A spatially fully distributed approach would include a completely different model structure and numerical approach, and require many more data. However, even in our spatially-lumped approach, some key notions such as hydrological connectivity between hillslopes and channels [e.g., *Reid et al*., 2007; *Fryirs*, 2013] may be included for instance by increasing the number of sediment reservoirs representing different landforms, redefining their connections, deposition rates, etc. These extensions, however, only make sense when they can be based on independent observations.

One of the key results of our model is that we can attribute the sediment discharge properties to a combination of stochasticity of sediment supply and the critical discharge threshold for debris flow generation. More specifically, the role of the discharge threshold Q_{df} in limiting the volume of discharge that can entrain and transport sediment is key for reproducing the distribution of event sizes as illustrated by the similarity of the distribution of debris flows generated by excess discharge events to the observed distribution (Figure 7). A stochastic sediment supply is needed to reproduce realistic sediment storage, supply limiting conditions, and ultimately sediment discharge properties (compare procedures 1–3 with 4–5 in Table 2). However, an important finding is that the actual triggering mechanism and timing of slope failures drawn from the probability distribution of slope failures (procedures 1–3) has a rather small influence on the shape of the final debris flow distribution. It appears that details of the sediment input are filtered out by the sediment cascade, runoff regime, and debris flow generation procedure. This result is of course valid only for our sediment cascade model and for the studied triggering mechanisms and time period in the Illgraben. It

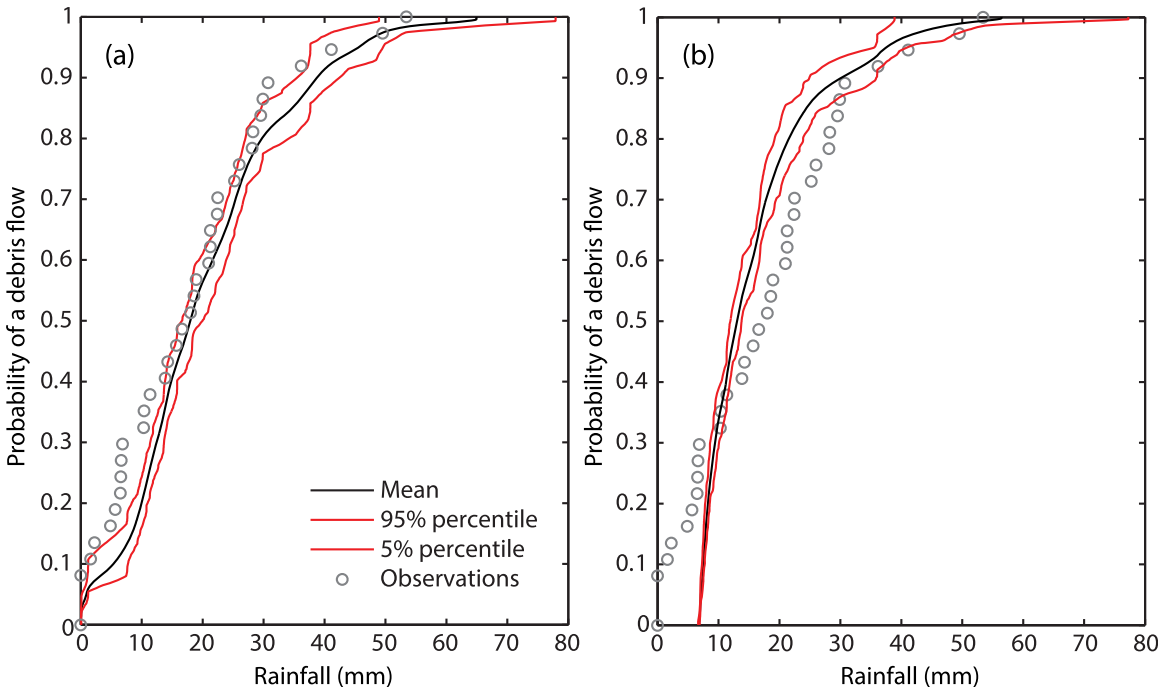

Figure 12. (a) Modeled (mean and 90% confidence bounds) and observed (36 events) probability distribution of daily rainfall on days with debris flows. (b) Modeled probability with rainfall triggering only, i.e., bypassing the hydrological model component. Simulations are for sediment input procedure (1).

may be that in other cases and over the long term, the signature of sediment input will be more identifiable in the sediment yield. Nevertheless, our study provides an example where the reconstruction of sediment input characteristics from yield data alone may be problematic [e.g., *Jerolmack and Paola*, 2010].

The model results in transport-limited behavior about 55% of the time, in line with descriptions of the Illgraben as a transport-limited system [*Schlunegger et al.*, 2009; *Bennett et al.*, 2012]. Nevertheless, it is the supply-limited condition in the channel (29–42% of the events were supply limited, 11–25% were prohibited from occurring altogether) that results in highly nonlinear sediment discharge as a function of runoff (Figure 9). However, because the distribution of the sediment discharge events is to some degree related to precipitation, especially for large events, we conclude that changes in the magnitude and frequency of precipitation may sometimes be inferred from sedimentary archives. This would not be the case if the distribution of sediment discharge only reflected the internal sediment storage dynamics of the system. We plan to evaluate the broader effects of changing precipitation forcing in the Illgraben by simulation with SedCas under different climate change and sediment supply scenarios in the future.

In our research, we also addressed the issue of the timing of debris flows and using rainfall as a deterministic predictor of debris flow occurrence. The triggering of slope failures is a complex phenomenon, with less clear controls than debris flows [*Bennett et al.*, 2013], making it impossible to reproduce the actual sediment supply and to accurately reproduce the daily timing of debris flows. The imperfect daily timing of modeled debris flows in our model may have a number of reasons in addition to the stochastic input by hillslope landslides. Foremost is that the areal averaging and daily time step mean that some localized storms with short duration high-intensity rainfall that led to debris flow cannot be simulated. Although we consider connectivity in the sense of accumulation and collapse of hillslope sediment storage, we do not consider blocking of debris flows by landslides in the channel [e.g., *Bardou et al.*, 2003] nor the propagation of landslides directly into debris flows [e.g., *Burtin et al.*, 2012]. The problem of overprediction of large debris flows by the model may be improved by including an additional fan reservoir that would account for redeposition or complete stopping of debris flows on the Illgraben fan [*Schürch et al.*, 2011]. However, it has to be stressed that our model is not an operational tool for debris flow forecasting. The main advantage lies not in the actual timing of events, but in the fact that the model predicts the probability of debris flow events for a range of rainfall magnitudes, and

therefore, inherently quantifies the uncertainty in using a rainfall threshold as an independent variable for debris flow triggering (compare Figures 12a and 12b). One possible application of the modeling approach is therefore to enhance rainfall magnitude-intensity threshold methods by making them seasonally dependent and conditioned on antecedent wetness and sediment storage.

6. Conclusions

We present a probabilistic sediment cascade model with the overall aim of explaining the nonlinear and stochastic sediment discharge from a mountain basin. We base this model on the Illgraben, a debris-flow prone catchment in the Swiss Alps, for which measurements of slope failures and debris flows spanning several years are available. The conceptual model consists of two sediment storage reservoirs representing hillslopes and channels and one water reservoir for the basin hydrology. Water and sediment are transferred between the reservoirs based on simple but physically meaningful rules. There are few parameters, most of which are estimated independently and not fine tuned to model output. Our main conclusions are as follows:

1. The model successfully reproduces the shape of the probability distribution and seasonal distribution of 36 observed debris flows from 2000 to 2009 driven by a deterministic climate and stochastic hillslope sediment input. Practically all observations are contained within the 90% confidence bounds of the simulations. The mean residence time of sediment in the channel and realistic ranges for volumetric concentration of sediment discharge events are also reproduced, all of which suggest that the model captures the essential sediment transfer behavior of the system at this scale.

2. The results show that the main control on the shape of the probability distribution of the volume of large debris flows is the threshold discharge parameter that defines discharge events with the potential to entrain and transport sediment and generate debris flows. The stochastic element of hillslope sediment input is important to reproduce realistic sediment storage and occasional supply-limiting conditions (29–42% of the events were supply limited and 11–25% were prevented from occurring altogether) that steepen the tail of the debris flow distribution. However, the triggering mechanism of slope failures (frost cracking, rainfall, or purely random occurrence) in our sediment cascade model all led to similar probability distributions of large debris flows, which suggests that details of the sediment input are filtered out by the system dynamics to the point that they may not be easily recovered from sediment output alone. Although this result is valid only for our sediment cascade model setup and its application to Illgraben, it corroborates observations in other geomorphic systems [e.g., *Jerolmack and Paola*, 2010].

3. Supply-limiting conditions produce a range of sediment concentrations for a discharge event of a given magnitude and sediment discharge events can be classified accordingly into floods, debris floods and debris flows. Additionally, the model generates debris flows for a wide range of rainfall magnitudes as a function of antecedent basin wetness conditions, demonstrating the importance of the hydrological model component, which includes snow cover and soil water storage dynamics. The model demonstrates the importance of considering both antecedent moisture and sediment storage for debris flow prediction and helps to understand the limitations of debris-flow predictions based on rainfall-triggering alone, e.g., the rainfall intensity-duration curve approach.

In summary, although the approach presented here describes the processes of sediment transfer and debris flow generation in a simplified conceptual manner, it produces complex sediment discharge behavior which can be explained only by considering jointly the availability of sediment, water, and the triggering potential, quantifying the role of history (system memory) and climate (triggering events) on sediment discharge in the Illgraben. Although this application was developed for the Illgraben, we believe the approach is reproducible in other mountain basins and the findings have general implications for fluvial systems that can be schematized into sediment cascades where the supply of sediment and triggering of events is largely stochastic.

Acknowledgments

This study was completed within the SedyMONT project, part of the ESF-funded TOPOEUROPE program. Funding provided by the Swiss National Science Foundation grants 20T021-120467 and 200020_144515 is acknowledged. Climatic input data were provided by MeteoSwiss (rainfall, temperature, radiation, and cloud cover) and the Institute of Snow and Avalanche Research of WSL (snow depth). Thanks to Bettina Schaeppi for her help with the model code. Reviews by J. Kean and two anonymous reviewers and editorial work by C. Ancey led to significant improvements of the manuscript.

References

Ancey, C., M. Meunier, and D. Richard (2003), The inverse problem for avalanche-dynamics models, *Water Resour. Res.*, *39*(4), 1099, doi: 10.1029/2002WR001749.

Bardou, E., and R. Delaloye (2004), Effects of ground freezing and snow avalanche deposits on debris flows in alpine environments, *Nat. Hazards Earth Syst. Sci.*, *4*, 519–530.

Bardou, E., and M. Jaboyedoff (2008), Debris flows as a factor of hillslope evolution controlled by a continuous or a pulse process?, *Geol. Soc. Spec. Publ.*, *296*, 63–78, doi:10.1144/SP296.5.
Bardou, E., F. Fournier, and M. Sartoir (2003), Palaeoflood reconstruction at Illgraben torrent (Switzerland): A current need for event frequency estimation, paper presented at Palaeofloods, Historical Floods and Climatic Variability: Applications in Flood Risk Assessment, edited by V. R. Thorndycraft, G. Benito, M. Barriendos, and M. C. Llasat, pp. 53–59, PHEFRA Workshop, Barcelona.
Badoux, A., C. Graf, J. Rhyner, R. Kuntner, and B. McArdell (2009), A debris-flow alarm system for the Alpine Illgraben catchment: Design and performance, *Nat. Hazards*, *49*(3), 517–539.
Benda, L., and T. Dunne (1997), Stochastic forcing of sediment supply to channel networks from landsliding and debris flow, *Water Resour. Res.*, *33*(12), 2849–2863.
Bennett, G. L. (2013), Quantifying and modeling sediment transfer through the Illgraben, PhD dissertation, 142 pp., ETH Zurich, Zurich, Switzerland.
Bennett, G. L., P. Molnar, H. Eisenbeiss, and B. W. McArdell (2012), Erosional power in the Swiss Alps: Characterization of slope failure in the Illgraben, *Earth Surf. Processes Landforms*, *37*(15), 1627–1640.
Bennett, G. L., P. Molnar, B. W. McArdell, F. Schlunegger, and P. Burlando (2013), Patterns and controls of sediment production, transfer and yield in the Illgraben, *Geomorphology*, *188*, 68–82, doi:10.1016/j.geomorph.2012.11.029.
Berger, C., B. W. McArdell, and F. Schlunegger (2011), Sediment transfer patterns at the Illgraben catchment, Switzerland: Implications for the time scales of debris flow activities, *Geomorphology*, *125*(3), 421–432.
Bovis, M. J., and M. Jakob (1999), The role of debris supply conditions in predicting debris flow activity, *Earth Surf. Processes Landforms*, *24*(11), 1039–1054.
Burt, T., and R. Allison (2010), Sediment cascades in the environment: An integrated approach, in *Sediment Cascades: An Integrated Approach*, pp. 1–16, Wiley-Blackwell, Chichester, U. K.
Burtin, A., N. Hovius, J. Turowski, B. McArdell, and J. Vergne (2012), High-resolution seismic monitoring of geomorphic activity in a catchment, *Geophys. Res. Abst. 14*, *EGU2012–11263*.
Carenzo, M., F. Pellicciotti, S. Rimkus, and P. Burlando (2009), Assessing the transferability and robustness of an enhanced temperature-index glacier-melt model, *J. Glaciol.*, *55*(190), 258–274.
Coulthard, T. J., and M. J. Van De Wiel (2007), Quantifying fluvial non linearity and finding self organized criticality? Insights from simulations of river basin evolution, *Geomorphology*, *91*(3–4), 216–235.
Coulthard, T. J., M. J. Kirkby, and M. G. Macklin (2000), Modelling geomorphic response to environmental change in an upland catchment, *Hydrol. Processes*, *14*(11–12), 2031–2045.
Eriksson, E. (1971), Compartment models and reservoir theory, *Ann. Rev. Ecol. Syst.*, *2*(1), 67–84.
Fatichi, S., S. Rimkus, P. Burlando, R. Bordoy, and P. Molnar (2013), Elevational dependence of climate change impacts on water resources in an Alpine catchment, *Hydrol. Earth Syst. Sci.*, *10*, 3743–3794.
Frei, C., and C. Schär (1998), A precipitation climatology of the Alps from high resolution raingauge observations, *Int. J. Climatol.*, *18*, 873–900.
Fryirs, K. (2013), (Dis)Connectivity in catchment sediment cascades: A fresh look at the sediment delivery problem, *Earth Surf. Processes Landforms*, *38*, 30–46.
Fuller, C. W., S. D. Willett, and N. Hovius (2003), Erosion rates for Taiwan mountain basins: New determinations from suspended sediment records and a stochastic model of their temporal variation, *J. Geol.*, *111*(1), 71–87.
Gabus, J. H., M. Weidmann, P.-C. Bugnon, M. Burri, M. Sartori, and M. Marthaler (2008), Feuille 1287 Sierre.—Atlas géol, Suisse 1:25 000, Notice expl. 111.Rep.
Jakob, M., M. Bovis, and M. Oden (2005), The significance of channel recharge rates for estimating debris-flow magnitude and frequency, *Earth Surf. Processes Landforms*, *30*(6), 755–766.
Jerolmack, D. J., and C. Paola (2010), Shredding of environmental signals by sediment transport, *Geophys. Res. Lett.*, *37*, L19401, doi: 10.1029/2010GL044638.
Keller, F., and H. U. Gubler (1993), Interaction between snow cover and high mountain permafrost, Murtèl-Corvatsch, Swiss Alps, in *Proceedings of the Sixth International Conference on Permafrost*, pp. 332–337, South China Univ. of Technol. Press, Beijing, China.
Kirchner, J. W. (2009), Catchments as simple dynamical systems: Catchment characterization, rainfall-runoff modeling, and doing hydrology backward, *Water Resour. Res.*, *45*, W02429, doi:10.1029/2008WR006912.
Lancaster, S. T., and N. E. Casebeer (2007), Sediment storage and evacuation in headwater valleys at the transition between debris-flow and fluvial processes, *Geology*, *35*(11), 1027–1030.
Lichtenhahn, C. (1971), Zwei Betonmauern: Die Geschieberückhaltesperre am Illgraben (Wallis) und die Staumauer des Hochwasserschutzbeckens an der Orlegna im Bergell (Graubünden), paper presented at International Symposium Interpraeents. pp. 451–463, Villach, Kaernten, Austria.
Lisle, T. E., and M. Church (2002), Sediment transport-storage relations for degrading, gravel bed channels, *Water Resour. Res.*, *38*(11), 1219, doi:10.1029/2001WR001086.
Lu, H., C. J. Moran, and M. Sivapalan (2005), A theoretical exploration of catchment-scale sediment deliver, *Water Resour. Res.*, *41*, W09415, doi:10.1029/2005WR004018.
Lu, H., C. J. Moran, and I. P. Prosser (2006), Modelling sediment delivery ratio over the Murray Darling Basin, *Environ. Model. Software*, *21*(9), 1297–1308.
Malmon, D. V., T. Dunne, and S. L. Reneau (2003), Stochastic theory of particle trajectories through alluvial valley floors, *J. Geol.*, *111*(5), 525–542.
McArdell, B. W., P. Bartelt, and J. Kowalski (2007), Field observations of basal forces and fluid pore pressure in a debris flow, *Geophys. Res. Lett.*, *34*, L07406, doi:10.1029/2006GL029183.
Molini, A., G. G. Katul, and A. Porporato (2011), Maximum discharge from snowmelt in a changing climate, *Geophys. Res. Lett.*, *38*, L05402, doi:10.1029/2010GL046477.
Molnar, P., P. Burlando, J. Kirsch, and E. Hinz (2006), Model investigations of the effects of land-use changes and forest damages on erosion in mountainous environments, *IAHS Publ.*, *306*, 589–600.
Nakamura, F., and S.-I. Kikuchi (1996), Some methodological developments in the analysis of sediment transport processes using age distribution of floodplain deposits, *Geomorphology*, *16*(2), 139–145.
Nydegger, C. (2008), *Fluvial System Dynamics in Steep Headwater Basins: A Study on the Illgraben Catchment*, 96 pp., ETH Zurich, Zurich, Switzerland.
Otto, J.-C., L. Schrott, M. Jaboyedoff, and R. Dikau (2009), Quantifying sediment storage in a high alpine valley (Turtmanntal, Switzerland), *Earth Surf. Processes Landforms*, *34*, 1726–1742.

Perona, P., A. Porporato, and L. Ridolfi (2007), A stochastic process for the interannual snow storage and melting dynamics, *J. Geophys. Res.*, *112*, D08107, doi:10.1029/2006JD007798.
Phillips, J. D. (2003), Alluvial storage and the long-term stability of sediment yields, *Basin Res.*, *15*(2), 153–163.
Phillips, J. D. (2006), Evolutionary geomorphology: Thresholds and nonlinearity in landform response to environmental change, *Hydrol. Earth Syst. Sci.*, *10*(5), 731–742.
Priestley, C. H. B., and R. J. Taylor (1972), On the assessment of surface heat flux and evaporation using large-scale parameters, *Mon. Weather Rev.*, *100*, 81–92.
Reid, S. C., S. N. Lane, D. R. Montgomery, and C. J. Brookes (2007), Does hydrological connectivity improve modelling of coarse sediment delivery in upland environments, *Geomorphology*, *90*, 263–282.
Rödder, T., and C. Kneisel (2012), Influence of snow cover and grain size on the ground thermal regime in the discontinuous permafrost zone, Swiss Alps, *Geomorphology*, *175*, 176–189, doi:10.1016/j.geomorph.2012.07.008.
Schlunegger, F., A. Badoux, B. W. McArdell, C. Gwerder, D. Schnydrig, D. Rieke-Zapp, and P. Molnar (2009), Limits of sediment transfer in an alpine debris-flow catchment, Illgraben, Switzerland, *Quat. Sci. Rev.*, *28*(11–12), 1097–1105.
Schumm, S. A. (1979), Geomorphic thresholds: The concept and its applications, *Trans. Inst. Br. Geogr.*, *4*(4), 485–515.
Schürch, P., A. L. Densmore, N. J. Rosser, and B. W. McArdell (2011), Dynamic controls on erosion and deposition on debris-flow fans, *Geology*, *39*(9), 827–830.
Stoffel, M., D. Conus, M. A. Grichting, I. Lièvre, and G. Maître (2008), Unraveling the patterns of late Holocene debris-flow activity on a cone in the Swiss Alps: Chronology, environment and implications for the future, *Global Planet. Change*, *60*(3–4), 222–234.
Theler, D., E. Reynard, C. Lambiel, and E. Bardou (2010), The contribution of geomorphological mapping to sediment transfer evaluation in small alpine catchments, *Geomorphology*, *124*, 113–123.
Tipper, J. C. (2007), The 'stochastic river': The use of budget-capacity modelling as a basis for predicting long-term properties of stratigraphic successions, *Sediment. Geol.*, *202*(1–2), 269–280.
Tucker, G., S. Lancaster, N. Gasparini, and R. L. Bras (2001), The channel-hillslope integrated landscape development model (CHILD), in *Landscape Erosion and Evolution Modeling*, edited by R. Harmon and W. W. Doe III, pp. 349–388, Kluwer Acad., New York.
Tuttle, S. E., and G. D. Salvucci (2012), A new method for calibrating a simple, watershed-scale model of evapotranspiration: Maximizing the correlation between observed streamflow and model-inferred storage, *Water Resour. Res.*, *48*, W05556, doi:10.1029/2011WR011189.
Van De Wiel, M. J., and T. J. Coulthard (2010), Self-organized criticality in river basins: Challenging sedimentary records of environmental change, *Geology*, *38*(1), 87–90.
Van De Wiel, M. J., T. J. Coulthard, M. G. Macklin, and J. Lewin (2011), Modelling the response of river systems to environmental change: Progress, problems and prospects for palaeo-environmental reconstructions, *Earth Sci. Rev.*, *104*(1–3), 167–185.
Walling, D. E. (1983), The sediment delivery problem, *J. Hydrol.*, *65*, 209–237.